Journal of Photochemistry & Photobiology, B: Biology 209 (2020) 111887

Contents lists available at ScienceDirect

Journal of Photochemistry & Photobiology, B: Biology

journal homepage: www.elsevier.com/locate/jphotobiol

A general framework for non-exponential delayed fluorescence and phosphorescence decay analysis, illustrated on Protoporphyrin IX

Gauthier Croizat[a,*], Aurélien Gregor[a], Emmanuel Gerelli[a], Jaroslava Joniova[a], Marek Scholz[b,*], Georges Wagnières[a]

[a] Laboratory for functional and metabolic imaging, LIFMET, Swiss Federal Institute of Technology (EPFL), Lausanne, Switzerland
[b] Faculty of Science, University of South Bohemia, České Budějovice, Czech Republic

ARTICLE INFO

Keywords:
Time-resolved spectroscopy
Delayed fluorescence
Phosphorescence
Triplet state kinetics
Cancer photodetection
Oxygen sensing

ABSTRACT

Delayed fluorescence (DF) is a long-lived luminescence process used in a variety of applications ranging from oxygen sensing in biological tissues to organic Light Emitting Diodes. In common cases, DF results from the de-excitation of the first excited triplet state via the first excited singlet state of the chromophore, which produces a mono-exponential light signal whose amplitude and lifetime give an insight into the probed environment. However, non-linear de-excitation reactions such as triplet-triplet annihilation, which can cause decays to lose their mono-exponential nature, are often neglected. In this work, we derive a global framework to properly interpret decays resulting from a combination of linear and non-linear de-excitation processes. We show why the standard method of using multi-exponential models when decays are not mono-exponential is not always relevant, nor accurate. First, we explain why the triplet de-excitation and light production processes should be analyzed individually: we introduce novel concepts to precisely describe these two processes, namely the de-activation pathway – the reaction which mainly contributes to the triplet state de-excitation – and the measurement pathway – the reaction which is responsible for light production. We derive explicit fitting functions which allow the experimenter to estimate the reaction rates and excited state concentrations in the system. To validate our formalism, we analyze the in vitro Transient Triplet Absorption and DF of Protoporphyrin IX, a well-known biological aromatic molecule used in photodynamic therapy, cancer photodetection and oxygen sensing, which produces DF through various mechanisms depending on concentration and excitation intensity. We also identify the precise assumptions necessary to conclude that triplet-triplet annihilation DF should follow a mono-exponential decay with a lifetime of half the triplet state lifetime. Finally, we describe why the commonly used definitions of triplet / DF lifetime are ill-defined in the case where second-order reactions contribute to the deactivation process, and why the fitting of precise mixed-orders DF kinetics should be preferred in this case. This work could allow the correct interpretation of various long-lived luminescence processes and facilitate their understanding.

1. Introduction

Delayed Fluorescence (DF) is a long-lived luminescence process performed by certain organic and inorganic aromatic molecules. It has been used for various applications, including oxygen partial pressure quantification in biological tissues [1–6] and effective light production in flexible Organic LEDs.

In general, delayed fluorescence is the result of four consecutive steps, illustrated by a simplified Jablonski diagram on Fig. 1. Depending on the nature of the reverse inter-system crossing (RISC) reaction, different types of DF can be identified [4,7]:

The simplest DF process is thermally activated and is called E-type DF (Eosin-type DF [7], also designated by TADF [8–10]). The corresponding reaction is: $T_1 \xrightarrow{k_B T} S_1$ followed by $S_1 \xrightarrow{h\nu} S_0$. It is a first order reaction, which dominates at low triplet state concentration (i.e. low chromophore concentration or low excitation intensity). The rate of E-type DF is proportional to the Boltzmann factor $\exp(-\Delta E/k_B T)$, where ΔE is the energy gap separating the T_1 and S_1 states. Therefore, higher temperature and lower $S_1 - T_1$ energy gap are favourable to E-type DF. For Protoporphyrin IX, $\Delta E = 35\ kJ.mol^{-1} = 0{,}36\ eV$, while $k_B T = 2{,}5$

Abbreviations: DF, delayed fluorescence; (R)ISC, (reverse) intersystem crossing; TTA, transient triplet absorption

* Corresponding authors.
E-mail addresses: g.croizat@gmail.com (G. Croizat), mara.scholz@gmail.com (M. Scholz).

https://doi.org/10.1016/j.jphotobiol.2020.111887
Received 12 February 2020; Received in revised form 14 April 2020; Accepted 26 April 2020
Available online 30 April 2020

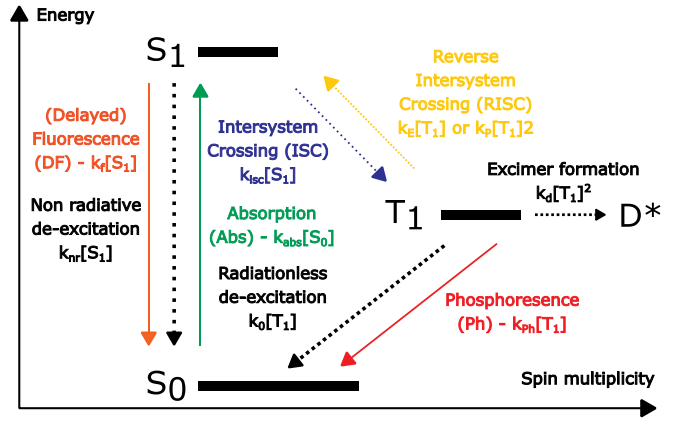

Fig. 1. Simplified Jablonski diagram of delayed fluorescence and phosphorescence, with the name and reaction rate of the corresponding processes. Dotted line: non-radiative, continuous line: radiative.

$kJ.mol^{-1} = 2{,}6 \times 10^{-2} eV$ at room temperature [11,12].

At higher triplet state concentration, a collision of two molecules in their triplet states becomes more probable, and can give rise to one excited S_1 molecule, and one relaxed to the ground state: $2T_1 \rightarrow S_1 + S_0$, which can be followed by DF: $S_1 \overset{h\nu}{\rightarrow} S_0$. This type of DF is called P-type DF (Pyrene-type DF [7], also termed Triplet-triplet Annihilation DF [13–16]). It is a second order reaction, as two T_1 molecules are involved.

- The presence of a triplet state quencher, typically oxygen, can provoke other forms of DF, such as Singlet Oxygen Feedback Delayed Fluorescence (SOFDF) [4,17]. Although they have been observed in organic and inorganic environments, we do not consider them in this work as we investigate the nature of DF and phosphorescence in absence of any triplet quencher.

1.1. Kinetic Equations of the System

As illustrated in Fig. 1, after light absorption, the concentrations of molecules in the T_1 and S_1 states evolve according to the following non-linear differential equations [16] (reaction rates defined in Fig. 1):

$$\begin{cases} \dfrac{\partial[T_1]}{\partial t} = k_{ISC}[S_1] - (k_{Ph} + k_0 + k_E)[T_1] - 2(k_P + k_d)[T_1]^2 \\ \dfrac{\partial[S_1]}{\partial t} = k_E[T_1] + k_P[T_1]^2 - (k_{ISC} + k_f + k_{nr})[S_1] \end{cases} \quad (1)$$

As such, this non-linear differential system does not have a simple analytic solution. But several simplifying assumptions can be made. First, the reactions of de-excitation of the singlet state are so much faster than those of formation (k_f; k_{nr}; $k_{ISC} \sim ns^{-1} >> k_E + k_P[T_1] \sim ms^{-1}$) that the steady-state approximation can be applied to $[S_1]$:

$$\frac{\partial[S_1]}{\partial t} \approx 0 \Rightarrow [S_1] \approx \frac{1}{k_f + k_{nr} + k_{ISC}}(k_E[T_1] + k_P[T_1]^2) \quad (2)$$

From this approximation, a simple expression for the DF signal can be extracted:

$$I_{DF}(t) = k_f[S_1] = \theta_f(k_E[T_1] + k_P[T_1]^2) \quad (3)$$

with $\theta_f = \frac{k_f}{k_f + k_{nr} + k_{ISC}}$ the fluorescence quantum yield of the S_1 state. From this expression, the contributions of E-type and P-type RISC to the DF signal can be clearly distinguished:

$$\begin{cases} I_{DF}^E(t) = \theta_f k_E[T_1] \\ I_{DF}^P(t) = \theta_f k_E[T_1]^2 \end{cases} \quad (4)$$

Additionally, we are not taking into account transient events when RISC is followed by ISC, and T_1 state is thus immediately recovered. These events lead to a reduction of the effective RISC rates k_E and k_P, but do not alter the shape of the T_1 state kinetics. At this point, we have reduced the system to a unique equation: the evolution of the triplet state concentration, that we call the deactivation equation, completely defines the DF signal.

$$\frac{\partial[T_1]}{\partial t} = -(k_{Ph} + k_0 + k_E)[T_1] - 2(k_P + k_d)[T_1]^2 \quad (5)$$

1.2. Different de-Excitation Scenarios

Starting from a deactivation equation where both first and second order reactions can play a role:

$$\frac{\partial[T_1]}{\partial t} = -a[T_1] - b[T_1]^2 \quad (6)$$

with a and b the first and second order reaction rate constants (in s^{-1} and $M^{-1}s^{-1}$ respectively), we can isolate three scenarios:

1.2.1. First-Order de-Excitation

If the deactivation is dominated by the first order reactions ($a \gg b[T_1]$), we get the common case where the triplet population evolves mono-exponentially:

$$[T_1](t) = [T_1]_0 \exp\left(\frac{-t}{\tau_T}\right) \quad (7)$$

with the triplet lifetime $\tau_T = \frac{1}{a} = \frac{1}{k_0 + k_{Ph} + k_E}$.

According to Eq. 4, the kinetics of E-type DF and P-type DF are then:

$$\begin{cases} I_{DF}^E(t) = \theta_f k_E[T_1]_0 \exp\left(\dfrac{-t}{\tau_T}\right) \\ I_{DF}^P(t) = \theta_f k_P[T_1]_0^2 \exp\left(\dfrac{-2t}{\tau_T}\right) \end{cases} \quad (8)$$

In such case, the last equation shows that the P-type DF signal is mono-exponential with a lifetime equal to half the triplet lifetime. This result, often used in practice, can be named the *half triplet lifetime rule*. We study the conditions of its validity in Section 3.3.

1.2.2. Second-Order de-Excitation

Assuming now that second-order reactions dominate ($a \ll b[T_1]$), the deactivation equation can be written:

$$\frac{\partial[T_1]}{\partial t} = -b[T_1]^2 \quad (9)$$

and the solution is the second-order decay [16]:

$$[T_1](t) = \frac{[T_1]_0}{1 + b[T_1]_0 t} \quad (10)$$

1.2.3. Mixed-Orders de-Excitation

Lastly, we can study the intermediate case when both first and second-order reactions play a significant part ($a \approx b[T_1]$), as has been done elsewhere [13]. This gives rise to the *mixed-orders decay*:

$$[T_1]^{mixed}(t) = \frac{a}{e^{at}\left(\frac{a}{[T_1]_0} + b\right) - b} \quad (11)$$

When setting either a or b to 0, the previous simpler forms are obtained (Eqs. (10) and (8), respectively). At short and long times, this yields the following approximations:

$$\begin{aligned} &[T_1]^{mixed}(t \rightarrow 0) \approx \frac{[T_1]_0}{1 + (a + b[T_1]_0)t} \approx \frac{[T_1]_0}{1 + b[T_1]_0 t} \; if \quad a \ll b[T_1]_0 \\ &[T_1]^{mixed}(t \rightarrow +\infty) \approx \frac{a[T_1]_0}{a + b[T_1]_0} e^{-at} \end{aligned} \quad (12)$$

The initial phase of a mixed-order decay is not mono-exponential, and can be controlled by the second-order process. On the contrary, at longer times, the decay becomes mono-exponential and the first-order process controls its lifetime. This result can have interesting consequences in practice: to focus on the second-order processes, one can fit only the beginning of the decay, whereas to capture the first-order processes, one can select the tail of the decay.

Note that these scenarios are not mutually exclusive: they rather occur sequentially, from second-order to first-order through mixed-orders deactivation. This could be one of the factors that contribute to the steeper decays at short times, which have been observed in literature, both in vitro and in vivo [18,19]. In any decay, when the triplet population approaches 0, first-order reactions are necessarily dominating and the first-order scenario applies.

In other words, the light signal created during the triplet de-excitation images the reactions which contribute to the triplet depopulation. However, the contribution of light-producing reactions may or may not form a significant part of the overall deactivation. Interpreting a luminescence signal without any consideration on the reactions responsible for the triplet deactivation is incomplete, if not misleading.

The previous reasoning emerges into an important notion about classification of processes leading to delayed emission (either DF or phosphorescence). (i) *A process that significantly contributes to the triplet state depopulation*, i.e. a reaction that has an appreciable weight in the deactivation equation (Eq. 5), can be called a “deactivation pathway”. (ii) *A reaction responsible for light production, which does not substantially de-excite T_1but only gives an image of its deactivation,* can be called a “measurement pathway”. Depending on the nature of each of these pathways, we can determine the triplet kinetics as well as the DF kinetics, as is done in Table 1, in appendix.

The reasoning above applies not only to delayed fluorescence, but also to phosphorescence. Phosphorescence is a first order measurement pathway that directly reproduces the triplet kinetics: $I_{phosph} \propto [T_1]$. As such, it can be a first, mixed, or second-order decay depending on the deactivation pathway, just as described in Table 1.

To confirm our predictions on non-mono-exponential decays, we present experimental results in the next sections.

2. Materials and Methods

Solutions of Protoporphyrin IX (PpIX, Fluka, > 99,5%) diluted in Dimethylsulfoxide (DMSO, Sigma Aldrich, > 99%) at concentrations ranging from 1 to 400 μM were studied. No aggregates were present in the samples, as confirmed by a strictly proportional evolution of the absorption intensity with concentration, and unchanged absorption and fluorescence spectral shape (data not shown).

2.1. Delayed Fluorescence (setup 1)

The solution was placed in a 1 cm pathlength quartz cuvette. Delayed fluorescence curves were acquired on a calibrated Horiba Fluorolog-3 spectrofluorometer, operated in a front face mode. The cuvette was illuminated by a pulsed Xenon lamp (pulse duration FWHM: 2 μs, ~ 3000 pulses per curve, pulse repetition rate: 30 Hz, illuminated surface: $5 \times 7\ mm^2$, excitation / emission bandwidths: 10/10 nm, excitation light filtered using two monochromators). The sample was excited at 405 nm, and the emission was collected at 630 nm, the main DF peak. The radiant exposure on the sample was $1{,}4\ \mu J.cm^{-2}$, or lower when placing neutral density filters in the excitation beam. The temperature of the sample cell was maintained at 32 °C using a Carry PCB-150 Peltier thermoregulator. The pO_2 was brought to zero ($pO_2 < 0{,}38\ mmHg$) by bubbling N_2 in the cuvette at a flow rate of 3 L/min, using a Brick gas mixer (Life Imaging Services, Reinach, Switzerland). The zone of bubbling was not illuminated by the excitation beam, and the samples were constantly stirred during measurements. Decays were fitted using Origin V8 (OriginLab, Northampton, Massachusetts) to custom functions using the built-in Levenberg-Marquardt algorithm. The delayed fluorescence signals were collected and fitted in the time range from 0,1 to 11 ms.

2.2. Transient Triplet Absorption (setup 2)

Transient triplet absorption curves were obtained using a nanosecond pump-probe technique. A pump beam at 420 nm was generated by a frequency-tripled Q-switched Nd:YAG laser (Ekspla NT-342, 355 nm, 50 Hz repetition rate) pumping an optical parametric oscillator (OPO) and yielding 5 ns pulses (FWHM), with a radiant exposure around $30\ \mu J.cm^{-2}$ (illuminated surface: $1\ cm^2$). For sample concentration under 50 μM, a 1 cm pathlength quartz cuvette was used, while a 1 mm one was used for the 400 μM sample. White light produced by a continuous wave halogen lamp was used as probe beam. The pump and probe beams were perpendicular to each other. The transmitted probe light was detected by a fast photomultiplier tube (R9910, Hamamatsu) at 450 nm, a wavelength chosen for its limited absorption by the ground state S_0 and strong absorption by the first excited triplet state T_1. The resulting signals were recorded and digitalized with a broad bandwidth digital oscilloscope (Tektronix, DPO 7254), with a typical averaging over 200 shots. Samples were nitrogen flushed before the measurement until all oxygen was removed.

3. Results

3.1. Transient Triplet Absorption

In order to study the dependence of the triplet state deactivation kinetics on the initial concentration of excited states, transient triplet absorption (TTA) kinetics of PpIX in DMSO at increasing concentrations were analyzed (Fig. 2). Fit models for different scenarios were introduced in Section 1.2. A constant offset y_0 was added to every function to accommodate for the background signal.

At a low concentration of PpIX (5 μM- Fig. 2, top), the TTA kinetics is close to mono-exponential (green: $R^2 = 0.991$), although the tail of the decay indicates that the offset parameter in the mono-exponential fit is probably somewhat overestimated. The mixed-orders function gives a slightly better fit (red: $R^2 = 0.992$) and reduced offset, indicating a subtle second-order influence at 5 μM already. Nevertheless, it can be still concluded that the decay is almost mono-exponential. This result, which corresponds to Eq. 7, shows that the triplet state deactivates mainly through a first order reaction, in this case radiationless de-excitation $T_1 \rightarrow S_0$, E-type RISC $T_1 \rightarrow S_1$, and phosphorescence, with a triplet lifetime $\tau_T = 0{,}6\ ms$, or equivalently $k_E + k_0 + k_{ph} = 1{,}6 \times 10^3 s^{-1}$.

At a higher concentration of PpIX (50 μM- Fig. 2, center), second-order deactivation reactions are expected to play a more important role. The triplet population decay is indeed far from mono-exponential. As suggested by our model, a mixed-order decay function (Eq. 11) nicely matches the triplet population (red: $R^2 = 0.999$), while a biexponential is slightly less accurate (blue: $R^2 = 0.998$). Pure first or second-order deactivation models (green and cyan) are clearly inaccurate. Under such experimental conditions (PpIX concentration and excitation intensity), the triplet de-excites through both first and second-order processes, thus producing a mixed-orders deactivation pattern. Although multi-exponential fitting could lead to a satisfactory fit, it is an incorrect model in this scenario, and would give misleading results, such as a false impression of multiple populations of triplet state with different lifetimes.

Finally, for a high concentration of PpIX (400 μM - Fig. 2, bottom), the TTA kinetics converges to a pure second-order deactivation (Eq. 10, cyan: $R^2 = 0.990$), suggesting that P-type RISC and excimer formation almost exclusively contribute to the triplet deactivation. In this case, the pure second-order function is completely superimposed with the mixed-orders function (the latter is therefore not shown). Again, the

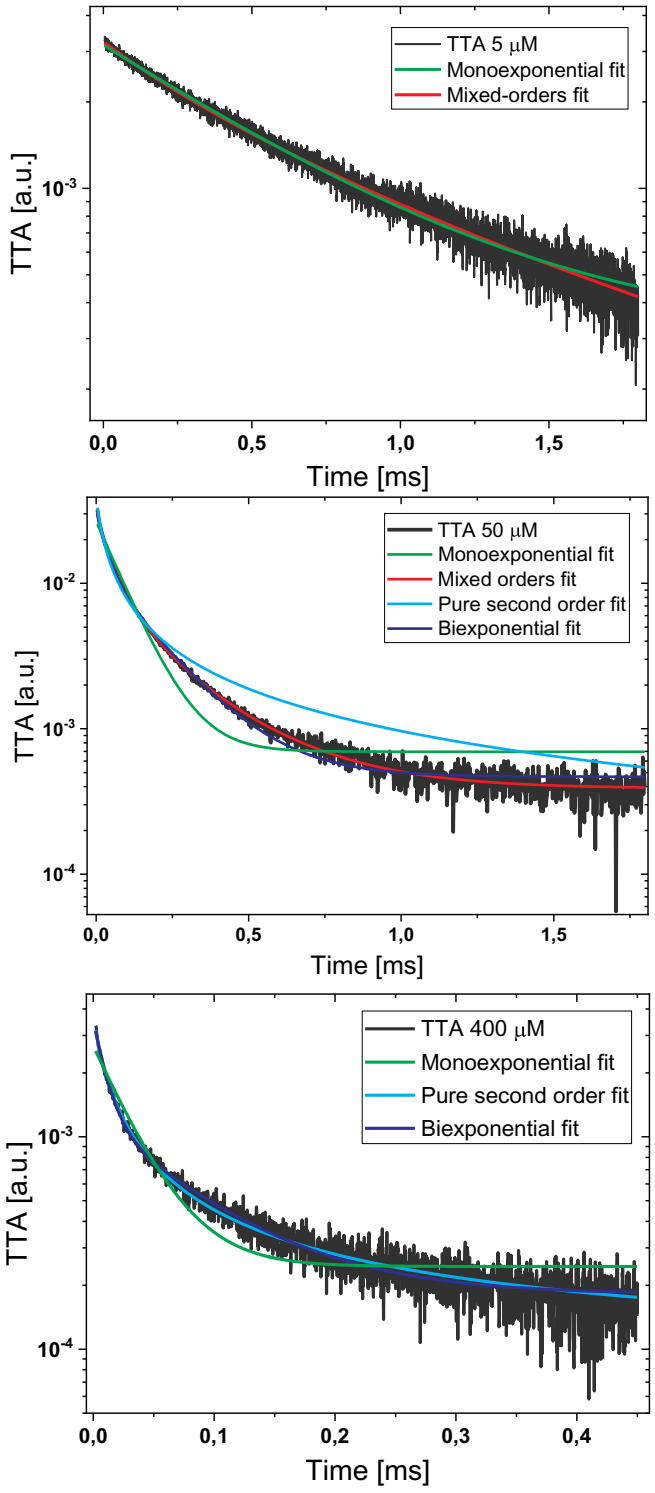

Fig. 2. Transient triplet absorption of PpIX in DMSO at 5 μM (top), 50 μM (center), and 400 μM (bottom), in semi-log scale. Different models have been used for fitting.

biexponential fit is slightly less precise (blue: $R^2 = 0.989$). We can extract values for $b = 2(k_P + k_d) \approx 3,4 \times 10^{10} M^{-1}s^{-1}$ and $[T_1]_0 = 2{,}6\ \mu M$. However, the mixed and second-order deactivation fit functions can suffer from interdependence of fitting parameters, which could be the reason for the quite large value of the parameter b obtained here. The reliability increases when some parameters are known a priori.

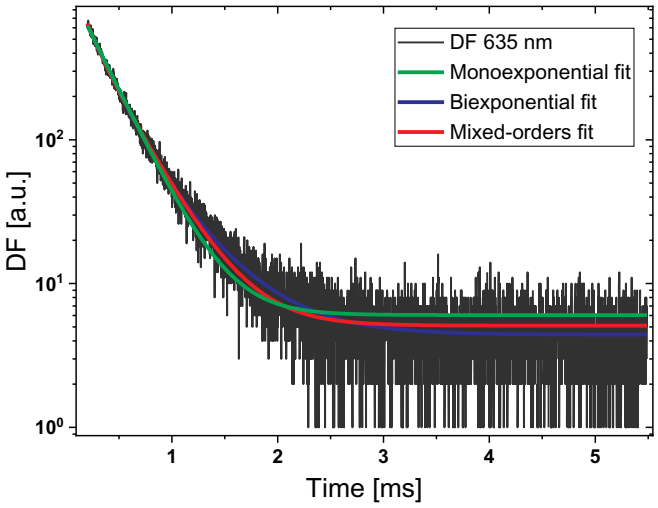

Fig. 3. DF of a sample of PpIX (50 μM) in DMSO, and corresponding fits, in semi-log scale.

Through this analysis, we have shown the full power of the deactivation pathway formalism, and illustrated the three different deactivation scenarios depending on the initial excited triplet concentration. We have shown that multi-exponential fitting was not the correct approach, as it could suggest the presence of several chromophores of distinct lifetimes, while it is in reality one chromophore which de-excites through various pathways. This illustrates the importance of determining the deactivation pathway for a correct interpretation of the decay kinetics.

3.2. Delayed Fluorescence

As detailed in part 1.2, the identification of the measurement pathway is also necessary to properly interpret a DF signal. Fig. 3 shows the DF kinetics of 50 μM PpIX in DMSO (setup 1). The decay is clearly not accurately fitted with a single exponential (green, $R^2 = 0.9940$). Although the DF curve shape could suggest a mixed-orders scenario, as in Fig. 2 – center, a closer look at the accuracy of each model indicates something different: contrary to the TTA at 50 μM, the precision of the biexponential fit (blue, $R^2 = 0.9949$) is better than the mixed-orders decay fit (red, $R^2 = 0.9947$), both visually and quantitatively, which disfavours the mixed-orders scenario. Moreover, the biexponential fit provides lifetimes $\tau_1 = 0{,}49\ ms$ and $\tau_2 = 0{,}23\ ms$. The ratio of the lifetimes is close to 2, which strongly suggests that the DF is produced by a mix of E-type, which produces a signal proportional to $e^{-t/\tau}$ (τ being the triplet lifetime), and P-type DF, which produces a signal proportional to $e^{-2t/\tau}$. In this case, against our first intuition, the analysis of the kinetics suggests that the triplet population decay is mono-exponential, with a lifetime $\tau_T = 0.49\ ms$, but the mixture of E-type and P-type DF creates a bi-exponential DF signal. Indeed, as detailed in Table 1, a bi-exponential DF signal can only be obtained if the triplet population decays mono-exponentially. This scenario corresponds to the half triplet lifetime rule described in Eq. 8 and Section 3.3. Note that, although the concentration of 50 μM is the same as in the TTA experiment in Fig. 2 (center), the triplet population remains mono-exponential in this case, because the excitation radiant exposure on this setup is about 20 times lower than that on the TTA setup. In this case, P-type DF is a measurement pathway, but not a significant deactivation pathway. Mixed-orders decays were not observed on this setup, due to insufficient excitation intensity. This graph illustrates the importance of identifying the measurement pathway before drawing any conclusions on the triplet deactivation.

3.3. The Half Triplet Lifetime Rule

Eq. 8 shows that P-type DF has a lifetime twice shorter than E-type DF in the same sample, with the same underlying *mono-exponential* triplet decay. However, it is quite common in literature to assume that the $\frac{1}{2}$ ratio between DF lifetimes of P-type and E-type DF also holds in samples with different concentration of triplet states, where E-type is a dominant measurement pathway at low concentrations of excited states or reduced singlet-triplet energy separation, while P-type becomes dominant at higher concentrations or higher energy separation [4,7,17,20–23]. However, as we have shown, samples at different concentrations (or excitation intensities) can have different triplet state lifetimes due to second-order decay processes. Based on the results above, we can conclude that the half triplet lifetime rule is only valid when the second-order P-type RISC is a measurement pathway, but not a deactivation pathway, in all the investigated samples. If P-type RISC is a deactivation pathway, then it shortens the triplet lifetime in the sample with higher concentration of excited states and also makes the triplet kinetics non-exponential. In other words, the half triplet lifetime rule applies in the range of triplet state concentration where P-type DF is detectable, but not strong enough to distort a mono-exponential decay. Nevertheless, in the case of non-exponential DF kinetics, the rule still applies to the mono-exponential part of the decay: if the initial non-exponential part is rejected, one can selectively fit a mono-exponential function to the remaining part of the decay. It is also important to note that if a shorter initial decay appears in DF kinetics at higher concentration of excited states, it should not necessarily be interpreted as the development of a $\frac{\tau_T}{2}$ exponential component, but, as shown in this paper, a mixed-orders deactivation should be considered.

3.4. Definition of Lifetime for Complex Decays

In many luminescence studies, the chromophore lifetime is a central part of the analysis. In the simple case where the deactivation and measurement pathways are of the first order, both triplet concentration and luminescence signal follow a mono-exponential function, whose characteristic time is defined as the inverse of the sum of the reaction rates: $\tau = \frac{1}{\sum k_i}$, which also appears as the time constant of the mono-exponential luminescence intensity: $I(t) = I_0 e^{-(\Sigma k_i)t}$. As such, τ is not a function of the chromophore concentration or excitation intensity: at first approximation, it can be considered as a fixed physical parameter, specific to the fluorescent molecule and its environment. It can be measured as a constant with a good repeatability, as it does not depend on the local fluence rate or chromophore concentration inhomogeneities. Its analysis provides a valuable insight into the system.

However, as we showed earlier, when a second order reaction (e.g. P-type RISC) also influences the deactivation, the reasoning is changed as the solution is no longer mono-exponential, and the definition of lifetime becomes challenging: the inverse of reaction rates becomes a variable parameter, the "instantaneous lifetime": $\tau_{instant} = \frac{1}{\sum k_i + 2k_P[T_1](t)}$.

When the triplet decay loses its mono-exponential nature, the triplet lifetime and luminescence lifetime have to be redefined, and it turns out that their values diverge. On the one hand, triplet lifetime can be most naturally expressed in the sense of a statistical expected value of deactivation time in the population of triplet states:

$$\tau_{T_1} = \frac{\int_0^{+\infty} t \frac{\partial [T_1]}{\partial t} dt}{\int_0^{+\infty} \frac{\partial [T_1]}{\partial t} dt} \tag{13}$$

On the other hand, the luminescence lifetime is in fact conceptually different: photons are created by deactivating molecules, and are almost instantaneously absorbed by the environment or the detector. Therefore, the definition of lifetime as expected value of the deactivation time introduced in Eq. 13 cannot be applied to the luminescence signal. Instead, the luminescence lifetime is defined as the expected value of the luminescence signal ([24], p.99), i.e. center of mass of the luminescence decay function:

$$\tau_{lum} = \frac{\int_0^{+\infty} t I_{lum}(t) dt}{\int_0^{+\infty} I_{lum}(t) dt} \tag{14}$$

The equality $\tau_{lum} = \tau_T$ is valid only if I_{lum} is proportional to $\frac{\partial [T_1]}{\partial t}$. In other words, only if both measurement and deactivation pathways are of the first order, which corresponds to a mono-exponential triplet decay scenario (Table 1). In any other case, DF and triplet lifetimes are different.

Injecting a mixed-orders function in definition 13, one can observe that when the first or second-order reaction rate constants a or b increase, the lifetime $\tau_T^{mixed\ orders}$ decreases, as expected, but when $[T_1]_0$ increases, the lifetime also diminishes, contrary to the mono-exponential case. Constants a and b cannot be determined from the value of the lifetime, even if $[T_1]_0$ is known. This analysis shows that when second-order processes are involved in the deactivation process, the triplet lifetime, understood as the life expectancy of an excited molecule in the triplet state, no longer corresponds to a physical constant linked to reaction rates, but depends on the initial triplet concentration $[T_1]_0$, which is a function of variable factors such as local chromophore concentration and excitation fluence rate. Additionally, when second-order deactivation or measurement pathways take place, DF and triplet lifetimes are no longer equal. For these two reasons, it appears that trying to infer a lifetime from a mixed-orders luminescence signal is not a relevant indicator of the system. Fitting one of the functions described in Table 1 is a more appropriate method to determine reaction rates and excited state concentration.

4. Discussion

Apart from providing a guidance in the interpretation of kinetics of DF, phosphorescence, and transient triplet absorption, the observations and formalism introduced in this work have interesting ramifications in the fields of photodynamic therapy (PDT) and organic LEDs:

In PDT, the intra and interpatient variations are a key obstacle. This is mostly due to the fact that the creation of singlet oxygen ($T_1 + {}^3O_2 \rightarrow S_0 + {}^1O_2$), which plays a key role in the mechanism leading to tissue damage, depends on the local fluence rate, pO_2 and photosensitizer concentration, i.e. variables that are frequently hard to estimate. To be more precise, the variables that will determine the quantity of singlet oxygen formed are the concentration of photosensitizer excited triplet state and the local concentration of oxygen. It is important to point out that this study only deals with situations where oxygen concentrations are low, which is relevant e.g. for PDT under hypoxic conditions. At higher oxygen levels, the quenching of triplets by oxygen introduces a strong competing deactivation pathway described by a rate equal to $k_q^{O2}[O_2][T_1]$. Therefore, this pathway falls into the first-order deactivation category, i.e. contributes to the "a" coefficient of Eq. 11, and the form of the fit function remains the same. Using our formalism, one could potentially deduce both the local photosensitizer and oxygen concentrations: the triplet decay rate at longer times reflects the rate of singlet oxygen production, while the non-exponentiality and decay rate at shorter times are controlled by the local triplet states concentration. Therefore, time-resolved measurement of the photosensitizer luminescence could help perform PDT dosimetry in a new fashion. In systems with higher oxygen concentrations, this estimation may become more complex due to the potential presence of singlet-oxygen-feedback delayed fluorescence [17], which is however beyond the scope of this work.

Interestingly, our results show that an excessive fluence rate leads to second-order de-excitation processes, which compete with first-order reactions like singlet oxygen formation. It is interesting to explore if this effect could be one of the reasons why PDT performed with identical light doses are frequently more potent with low rather than high

fluence rates (e.g. continuous versus pulsed excitation). Fig. 2 showed that pulsed excitation with radiant exposure $H_p = 30\ \mu J.cm^{-2}$ per pulse in a 50 μM PpIX solution induced pronounced triplet-triplet annihilation. Assuming a first-order triplet deactivation rate of $k = 2,0 \times 10^3 s^{-1}$ (lifetime of 0,50 *ms*), which would correspond to hypoxic conditions [25], it can be deduced that continuous irradiation with irradiance $I_c = kH_p = 60\ mW.cm^{-2}$ in the same sample would also lead to strong triplet-triplet deactivation effects. For comparison, the irradiances used in continuous PDT are ~10 $mW.cm^{-2}$ with blue excitation [26].

It is hard to answer whether a PpIX concentration of 50 μM is realistic in PDT. It has to be stressed that 50 μM refers here to the local concentration in the sites of subcellular accumulation (namely mitochondrial membranes), which is several orders of magnitude larger than the average tissular concentration [27,28]. Taking this into account, it is imaginable that the local mitochondrial PpIX concentration in lesions with a good production of PpIX could reach tens or hundreds of micromolar. However, the issue of determining the local mitochondrial PpIX concentration has not been resolved yet to the best of our knowledge, and this therefore remains an open question. Ideally, singlet oxygen production should be the only deactivation pathway for the photosensitizer triplet, which requires to keep the fluence rate and the resulting triplet state concentration low enough to avoid ineffective second-order de-excitation. One could increase the excitation intensity until the first signs of non-exponentiality in the DF or phosphorescence of the photosensitizer, and choose an excitation intensity just below that.

Conversely, in the field of organic LEDs, delayed fluorescence is used to harvest light energy from triplet states which would otherwise act as dark states that lower the light-emitting efficiency [8]. E-type DF pathway is preferable in LED devices, because in P-type DF only 50% of the reacting triplets undergo RISC. However, the rate of E-type DF rapidly drops with the increasing singlet-triplet energy gap and it may prove inefficient in competition with non-radiative triplet deactivation pathways. Analysis methods presented here could be used to study the mechanisms and rates of different triplet deactivation pathways and thus could help optimize the efficiency of the triplet energy retrieval.

5. Conclusion

In this work, we have developed a general framework for the analysis of delayed fluorescence, phosphorescence and transient triplet absorption kinetics, including situations where the kinetics are not exponential due to second-order deactivation processes such as triplet-triplet annihilation. We used Protoporphyrin IX in solution as an important illustrative example. It was shown that kinetics indeed become non-exponential and shorter-lived when higher concentrations of excited states were present. Non-exponential fitting models must be employed instead of multi-exponential ones, which could give a false impression of several chromophores of distinct lifetimes, while the decay corresponds to a single chromophore deactivating through several pathways. Further, we detailed the relationship between triplet kinetics and DF signals at different ranges of excited triplet state concentration. We showed the importance of uncoupling the analysis of the triplet deactivation and light production reactions, and introduced the deactivation and measurement pathways formalism to facilitate this analysis. The limits of validity of the half triplet lifetime rule for P-type DF have been discussed, and finally the meaning and relationship between DF and triplet lifetime in the case of nonlinear decays have been investigated. This work can serve as theoretical basis for the analysis of delayed fluorescence, phosphorescence and triplet state kinetics, and facilitate the correct interpretation of experimental data.

Funding & Acknowledgements

This work was supported by the Swiss National Science Foundation (Grant 315230_185262/1) and European Regional Development Fund (Project CZ.02.1.01/0.0/0.0/15_003/0000441). We would like to thank Prof. Jacques Moser for giving us access to the Transient Triplet Absorption setup.

Declaration of Competing Interest

The authors declare that they have no known competing financial interests or personal relationships that could have appeared to influence the work reported in this paper.

Appendix A

Table 1
Summary of the different DF kinetics depending on the deactivation and measurement pathways.

Deactivation pathway	Measurement pathway		
	E-type DF	P-type DF	Phosphorescence
	$I_{DF}^{E} = \theta_f k_E [T_1](t)$	$I_{DF}^{P} = \theta_f k_P [T_1](t)^2$	$I_{Ph} = k_{ph}[T_1](t)$
1st order: $\frac{\partial[T_1]}{\partial t} = -a[T_1]$	$I_{DF}^{E} = \theta_f k_E [T_1]_0 e^{-at}$	$I_{DF}^{P} = \theta_f k_P [T_1]_0^2 e^{-2at}$	$I_{Ph} = k_{ph}[T_1]_0 e^{-at}$
2nd order: $\frac{\partial[T_1]}{\partial t} = -b[T_1]^2$	$I_{DF}^{E} = \theta_f k_E \frac{[T_1]_0}{1+b[T_1]_0 t}$	$I_{DF}^{P} = \theta_f k_P \left(\frac{[T_1]_0}{1+b[T_1]_0 t}\right)^2$	$I_{Ph} = k_{ph}\frac{[T_1]_0}{1+b[T_1]_0 t}$
Mixed-orders: $\frac{\partial[T_1]}{\partial t} = -a[T_1] - b[T_1]^2$	$I_{DF}^{E} = \theta_f k_E \frac{a}{e^{at}\left(\frac{a}{[T_1]_0}+b\right)-b}$	$I_{DF}^{P} = \theta_f k_P \left(\frac{a}{e^{at}\left(\frac{a}{[T_1]_0}+b\right)-b}\right)^2$	$I_{Ph} = k_{ph}\frac{a}{e^{at}\left(\frac{a}{[T_1]_0}+b\right)-b}$

References

[1] F.A. Harms, E.G. Mik, In Vivo Assessment of Mitochondrial Oxygen Consumption, Humana Press, New York, NY, 2015, pp. 219–229, https://doi.org/10.1007/978-1-4939-2257-4_20.
[2] F.A. Harms, W.M.I. de Boon, G.M. Balestra, S.I.A. Bodmer, T. Johannes, R.J. Stolker, E.G. Mik, Oxygen-dependent delayed fluorescence measured in skin after topical application of 5-aminolevulinic acid, J. Biophotonics 4 (2011) 731–739, https://doi.org/10.1002/jbio.201100040.
[3] M. Scholz, A.-L. Biehl, R. Dědic, J. Hála, The singlet-oxygen-sensitized delayed fluorescence in mammalian cells: a time-resolved microscopy approach, Photochem. Photobiol. Sci. 14 (2015) 700–713, https://doi.org/10.1039/C4PP00339J.
[4] M. Scholz, R. Dědic, Singlet oxygen-sensitized delayed fluorescence, Singlet Oxyg. Delayed Fluoresc. (2016) 63–81, https://doi.org/10.1039/9781782626978-00063.
[5] E.G. Mik, J. Stap, M. Sinaasappel, J.F. Beek, J.A. Aten, T.G. van Leeuwen, C. Ince, Mitochondrial PO2 measured by delayed fluorescence of endogenous protoporphyrin IX, Nat. Methods 3 (2006) 939–945, https://doi.org/10.1038/nmeth940.
[6] F. Piffaretti, A.M. Novello, R.S. Kumar, E. Forte, C. Paulou, P. Nowak-Sliwinska,

H. van den Bergh, G. Wagnières, Real-time, in vivo measurement of tissular pO2 through the delayed fluorescence of endogenous protoporphyrin IX during photodynamic therapy, J. Biomed. Opt. 17 (2012) 115007, https://doi.org/10.1117/1.JBO.17.11.115007.

[7] C.A. Parker, C.G. Hatchard, Delayed fluorescence from solutions of anthracene and phenanthrene, Proc. R. Soc. A Math. Phys. Eng. Sci. 269 (1962) 574–584, https://doi.org/10.1098/rspa.1962.0197.

[8] H. Uoyama, K. Goushi, K. Shizu, H. Nomura, C. Adachi, Highly efficient organic light-emitting diodes from delayed fluorescence, Nature 492 (2012), https://doi.org/10.1038/nature11687.

[9] Q. Zhang, B. Li, S. Huang, H. Nomura, H. Tanaka, C. Adachi, Efficient blue organic light-emitting diodes employing thermally activated delayed fluorescence, (2014), https://doi.org/10.1038/NPHOTON.2014.12.

[10] H. Tanaka, K. Shizu, H. Miyazaki, C. Adachi, Efficient green thermally activated delayed fluorescence (TADF) from a phenoxazine–triphenyltriazine (PXZ–TRZ) derivative, Chem. Commun. 48 (2012) 11392, https://doi.org/10.1039/c2cc36237f.

[11] A. Suisalu, R. Avarmaa, Phosphorescence-detected triplet state microwave resonance of a protoporphyrin molecule in n-octane, Chem. Phys. Lett. 101 (1983) 182–186, https://doi.org/10.1016/0009-2614(83)87367-9.

[12] M. Gouterman, G.-E. Khalil, Porphyrin free base phosphorescence, J. Mol. Spectrosc. 53 (1974) 88–100, https://doi.org/10.1016/0022-2852(74)90263-X.

[13] M.A. Baldo, C. Adachi, S.R. Forrest, Transient analysis of organic electrophosphorescence. II. Transient analysis of triplet-triplet annihilation, Phys. Rev. B 62 (2000) 10967–10977, https://doi.org/10.1103/PhysRevB.62.10967.

[14] W.L. Peticolas, J.P. Goldsborough, K.E. Rieckhoff, Double photon excitation in organic crystals, Phys. Rev. Lett. 10 (1963) 43–45, https://doi.org/10.1103/PhysRevLett.10.43.

[15] R.G. Kepler, J.C. Caris, P. Avakian, E. Abramson, Triplet excitons and delayed fluorescence in anthracene crystals, Phys. Rev. Lett. 10 (1963) 400–402, https://doi.org/10.1103/PhysRevLett.10.400.

[16] A. Hayer, B. Bässler, S. Falk, Schrader, delayed fluorescence and phosphorescence from Polyphenylquinoxalines, J. Phys. Chem. A 106 (2002) 11045–11053, https://doi.org/10.1021/jp0214110.

[17] I.S. Vinklárek, M. Scholz, R. Dědic, J. Hála, Singlet oxygen feedback delayed fluorescence of protoporphyrin IX in organic solutions, Photochem. Photobiol. Sci. 16 (2017) 507–518, https://doi.org/10.1039/C6PP00298F.

[18] M. Scholz, X. Cao, J. Gunn, P. Brža, B. Pogue, Title: pO2-Weighted Imaging in Vivo by Delayed Fluorescence of Intracellular Protoporphyrin IX, (n.d.). doi:https://doi.org/10.1364/OL.99.099999.

[19] E.G. Mik, T. Johannes, C.J. Zuurbier, A. Heinen, J.H.P.M. Houben-Weerts, G.M. Balestra, J. Stap, J.F. Beek, C. Ince, In vivo mitochondrial oxygen tension measured by a delayed fluorescence lifetime technique, Biophys. J. 95 (2008) 3977–3990, https://doi.org/10.1529/BIOPHYSJ.107.126094.

[20] D.H. Volman, Advances in Photochemistry, Vol. 2 John Wiley & Sons, Inc., Hoboken, NJ, USA, 1964, https://doi.org/10.1002/9780470133323.

[21] J.B. Birks, G.F. Moore, I.H. Munro, Delayed excimer fluorescence, Spectrochim. Acta 22 (1966) 323–331, https://doi.org/10.1016/0371-1951(66)80241-2.

[22] G. Porter, M.R. Wright, Modes of energy transfer from excited and unstable ionized states. Intramolecular and intermolecular energy conversion involving change of multiplicity, Discuss. Faraday Soc. 27 (1959) 18, https://doi.org/10.1039/df9592700018.

[23] C.A. Parker, C.G. Hatchard, T.A. Joyce, P-type delayed fluorescence from ionic species and aromatic hydrocarbons, J. Mol. Spectrosc. 14 (1964) 311–319, https://doi.org/10.1016/0022-2852(64)90126-2.

[24] J.R. Lakowicz, Principles of Fluorescence Spectroscopy, Springer, 2006, https://doi.org/10.1007/978-0-387-46312-4.

[25] M. Scholz, A. Petusseau, J.R. Gunn, M.S. Chapman, B.W. Pogue, Imaging of hypoxia, oxygen consumption and recovery in vivo during ALA-photodynamic therapy using delayed fluorescence of Protoporphyrin IX, Photodiagn. Photodyn. Ther. (2020) Submitted for publication.

[26] T.H. Wong, C.A. Morton, N. Collier, A. Haylett, S. Ibbotson, K.E. McKenna, R. Mallipeddi, H. Moseley, D.C. Seukeran, L.E. Rhodes, K.A. Ward, M.F. Mohd Mustapa, L.S. Exton, P.M. McHenry, T.A. Leslie, S. Wakelin, R.Y.P. Hunasehally, M. Cork, G.A. Johnston, F.S. Worsnop, P. Rakvit, A. Salim, B. McDonald, S.L. Chua, D. Buckley, G. Petrof, N. Callachand, T. Flavell, A.A. Salad, British Association of Dermatologists and British Photodermatology Group guidelines for topical photodynamic therapy 2018, Br. J. Dermatol. 180 (2019) 730–739, https://doi.org/10.1111/bjd.17309.

[27] R. Chen, Z. Huang, G. Chen, Y. Li, X. Chen, J. Chen, H. Zeng, Kinetics and subcellular localization of 5-ALA-induced PpIX in DHL cells via two-photon excitation fluorescence microscopy, Int. J. Oncol. 32 (2008) 861–867, https://doi.org/10.3892/ijo.32.4.861.

[28] Z. Ji, G. Yang, V. Vasovic, B. Cunderlikova, Z. Suo, J.M. Nesland, Q. Peng, Subcellular localization pattern of protoporphyrin IX is an important determinant for its photodynamic efficiency of human carcinoma and normal cell lines, J. Photochem. Photobiol. B Biol. 84 (2006) 213–220, https://doi.org/10.1016/j.jphotobiol.2006.03.006.